

Self-healing of concrete cracks by the release of embedded water repellent agents and corrosion inhibitors to reduce the risk for reinforcement corrosion

VAN TITTELBOOM Kim^{1,a,*}, KESSLER Sylvia^{2,b}, DE MAESSCHALCK Claudia^{1,c}, VAN BELLEGHEM Bjorn^{1,3,d}, VAN DEN HEEDE Philip^{1,3,e} and DE BELIE Nele^{1,f}

¹Magnel Laboratory for Concrete Research, Ghent University, Faculty of Engineering and Architecture, Department of Structural Engineering, Technologiepark-Zwijnaarde 904, 9052 Ghent, Belgium

²Centrum Baustoffe und Materialprüfung, Technische Universität München, Ingenieur fakultät Bau Geo Umwelt, Baumbachstrasse 7, 81245 München, Germany

³Strategic Initiative Materials (SIM vzw), project ISHECO within the program 'SHE', SIM vzw, Technologiepark-Zwijnaarde 935, 9052 Ghent, Belgium

^akim.vantittelboom@ugent.be, ^bsylvia.kessler@tum.de, ^cclaudia.demaesschalck@ugent.be, ^dbjorn.vanbelleghem@ugent.be, ^ephilip.vandenheede@ugent.be, ^fnele.debelie@ugent.be

*corresponding author

Keywords: Self-repair, Encapsulation, Water repellent agent, Corrosion inhibitor, Reinforcement corrosion

Abstract. From the worldwide steel production, approximately 50 per cent is required to replace corroded steel [1]. In the case of reinforced concrete structures, corrosion of the reinforcement steel causes crack formation and spalling which leads to serviceability problems. Especially when small cracks are already present in the cementitious matrix in combination with aggressive ions present within the environment, a high risk for corrosion exists. Therefore, regular inspection, maintenance and crack repair are insurmountable for concrete structures. However, costs related to repair works mount up as not only the direct costs of the repair but also the indirect costs resulting from traffic jams and possible loss in productivity need to be taken into account. Self-repair of concrete cracks will have a high economic benefit as the indirect costs as well as a part of the direct costs can be avoided. In addition, it is assumed that self-repair will lead to more durable concrete structures as the risk for reinforcement corrosion may be decreased.

The possibility to implement self-healing properties in concrete has been investigated for several years now. One of the studied self-healing approaches relies on the use of encapsulated healing agents which are embedded in the matrix. When cracks appear, the capsules break and the healing agent is released in the crack, causing crack repair. In previous research [2, 3] it was shown that by using this approach, part of the mechanical properties and the water tightness of cracks was restored. In this study we investigate whether by encapsulation and embedment of a water repellent agent (WRA) and/or a corrosion inhibitor (CI), we can reduce the risk for reinforcement corrosion. A selection of WRA and/or CI were encapsulated and embedded inside reinforced concrete beams which were cracked to trigger the self-healing mechanism. By electrochemical measurements it was shown that the risk for reinforcement corrosion was reduced in comparison to untreated cracks when the cracked beams, containing encapsulated WRA and/or CI, were exposed to a chloride solution.

Introduction

Concrete easily cracks due to its rather low tensile strength. While some micro-cracks are already present in the material from the start, other cracks are formed when the concrete structure is subjected to loads or environmental conditions. For visible cracks running till the reinforcement level, the corrosion initiation will only require a brief period compared to the entire life time of the structure [4]. However, after the brief initiation period the corrosion rate is rather low as most concrete structures are cracked while they do not fail immediately. This low corrosion rate can be ascribed to autogenous healing of the cracks by unhydrated cement particles and precipitation of CaCO_3 . Another reason for this low corrosion rate might be the fact that the critical factors, needed for the corrosion reaction, are not always present. However, whether the afore-mentioned statement is valid will depend on several factors like the crack width, crack depth, environmental conditions, etc.

It is well known that cracks reduce the durability of concrete by creating preferential pathways for the penetration of various types of potentially aggressive agents [5-8]. Chlorides and carbonation of the concrete affect the durability of concrete by initiating corrosion of the reinforcement steel. Vaysburd and Emmons [9] stated that coefficients of carbon dioxide ingress are found which are three orders of magnitude higher for samples with a crack width of 0.2 mm compared to uncracked concrete. Also aggressive ions such as chloride ions will be more easily transported to the reinforcement as the capillary suction increases. The crack width is a key parameter controlling the local transport of chloride ions in a crack [10]. Generally, it is assumed that smaller cracks are of less importance with respect to durability than larger cracks. Several researchers [6, 8, 11] found that no significant chloride diffusion occurs in cracks having an opening below a critical value (0.012 - 0.030 mm). For cracks with a width larger than 0.2 mm, the diffusion of chlorides is not a limiting factor controlling the diffusion process perpendicular to the crack wall [8]. In addition, Win et al. [5] found that the penetration depth from the surface of the crack and the crack tip is equal to or slightly higher than that from the exposed surface, even for cracks with a width of 0.1 mm. Win et al. [5] also studied reinforced concrete specimens. When the chloride penetration reached the steel, penetration occurred all around the rebar, since the steel-concrete interface is usually more porous. Another important crack parameter that affects chloride penetration is the crack depth. Audenaert et al. [12] and Marsavina et al. [13] reported a higher chloride penetration depth for a higher crack depth. But Marsavina et al. [13] found that the distance between the crack tip and the chloride penetration front decreased for increasing crack depths.

Montes et al. [14] noticed that the rate of corrosion for cracked concrete was up to ten times higher than for uncracked concrete, for crack widths of 0.25 mm to 0.50 mm. Scott and Alexander [15] concluded that a wider crack width of 0.7 mm versus 0.2 mm, is responsible for a higher corrosion rate. Otieno et al. [16] found that crack widths of 0.4 and 0.7 mm result in corrosion rates that exceed the active corrosion threshold of $0.1 \mu\text{A}/\text{cm}^2$ suggested by Andrade and Alonso [17]. Samples with just incipient cracks – cracks visible under a mechanical load, but invisible after removal of the load – usually remain within the passive corrosion state. Beeby [18] observed only legible increases in corrosion rate with increasing crack width. Crack widths of 0.13, 0.25, 0.51 and 1.27 mm resulted in average depths of corrosion on the steel surface of 0.16, 0.16, 0.18 and 0.21 mm, respectively.

Use of corrosion inhibitors is one of the methods to protect the reinforcement against corrosion [19]. One can make a distinction between different corrosion inhibitors based on the type of product, the mechanism or the application manner. While some of the inhibitors are applied by adding them to the concrete mix, others are applied by impregnation at the surface and need to penetrate. While adding the inhibitor to the mixing water leads to an easy handling, these products

frequently affect the properties of the concrete unfavorably leading to increased setting times or decreased compressive strength. Applying inhibitors on the concrete surface might be a promising technique but the penetrability is mostly an issue leading to an insufficient molar concentration ratio between inhibitor and chlorides [20].

Hydrophobising concrete by applying water repellent agents could lead to a more durable structure. As concrete is a porous material, pores can contain water which affects the durability. Mainly the application of coatings or the impregnation with silanes and siloxanes are used for this purpose. Silanes can be added to the concrete mix or applied as a surface treatment. In Zhu et al. [21] the surface treatment was more effective than an integral water repellent concrete to reduce the capillary water absorption and penetration of aggressive substances. Largest improvements with addition of the silane-based water-repellent agents were noted for more porous concrete. The capillary suction will allow for the water repellent agent to be transported through the concrete. The use of hydrophobised concrete will reduce the chloride ingress. A beneficial effect would be the drying of the concrete by the use of water repellent agents as this would lead to a slowed down initiation phase. However, this extreme also leads to increased carbon dioxide diffusion.

Within the current study we aim to combine the advantages of both water repellent agents and corrosion inhibitors, while we try to overcome the afore mentioned limitations of each of them. In order to make sure that we have a high concentration of the inhibitor at the location of the steel reinforcement without having the need to influence the properties of the concrete we aim to embed WRA and/or CI inside capsules which are located close to the reinforcement bar. At the moment of concrete hardening the agents do not come into contact with the concrete and thus do not have an influence on the properties, however, at the moment of crack formation, the capsules break and release their content in the vicinity of the rebar leading to a possible reduced corrosion risk for the steel reinforcement.

Materials

Water repellent agents and corrosion inhibitors. In order to protect the steel reinforcement against corrosion encapsulated water repellent agents (WRA) and/or corrosion inhibitors (CI) were used. As it is the aim within this study to release the WRA and/or CI agents from embedded capsules, only fluids and soluble products were considered. Most of these products were commercially available, except the saturated sodium nitrite solution. Table 1 gives an overview of the used product(s) (types), their supplier, their standard application method and the active compound causing the water repellent or corrosion inhibiting effect. MasterProtect 8000 CI is an organofunctional silane based CI combining the properties of penetrative silane treatments for the control of moisture and chloride ion ingress with those of organofunctional CI. The product can be used as preventive measure or in the framework of a repair strategy. The product Ferrogard 901 S consists of a combination of organic CI and forms a film on the steel surface which delays the onset of corrosion and reduces the corrosion rate by reducing the anodic and cathodic reactions of the electrochemical corrosion process. Sikagard 705 L is a hydrophobic impregnation product. Ferrogard 903 Plus is a product based on organic compounds which forms a protective monomolecular layer on the steel surface delaying the start of corrosion and reducing the corrosion rate. Sodium nitrite is an inorganic corrosion inhibitor inhibiting the anodic reaction. It reacts with ferrous ions at the anode to form ferric oxide [20].

Table 1. Water repellent agents and corrosion inhibitors used within this study.

Product	Type	Supplier	Application method*	Active compound
MasterProtect 8000 CI	CI & WRA	BASF	Impregnation	Silanes
Ferrogard 901 S	CI	SIKA	Admixed	Amino alcohols
Sikagard 705 L	WRA	SIKA	Impregnation	Silanes
Ferrogard 903 Plus	CI	SIKA	Impregnation	Amino alcohols
Sodium nitrite	CI	-	Admixed	NaNO ₂

* Standard method of application

Capsules. Hollow borosilicate glass capillaries with an inner diameter of $3 \text{ mm} \pm 0.05 \text{ mm}$, a wall thickness of $0.175 \text{ mm} \pm 0.03 \text{ mm}$ and a length of 50 mm were used. One side of the capsules was sealed with 2-component polymethylmethacrylate (PMMA) glue and subsequently the WRA and/or CI were injected into these capsules by means of a syringe with a needle. Finally, the other end of the capsules was also sealed with PMMA.

Concrete specimens. Concrete beams with dimensions of $120 \text{ mm} \times 120 \text{ mm} \times 500 \text{ mm}$ were prepared. The reinforcement scheme can be found in Figure 1 and is based on the configuration used by Hiemer et al. [20, 21]. Two reinforcement cages at both sides of the beam were used as cathodic area and one single rebar in the middle was purposed to be the anode. The cathodic reinforcement cages were made by ribbed bars ($\varnothing 6 \text{ mm}$) as stirrups connected by four ribbed bars ($\varnothing 8 \text{ mm}$). The connection between the stirrups and the bars in the corners was made through wire connections in combination with welding to ensure a good electrical connection. In addition, an electrical connection was made between both cages by means of an insulated copper wire. A 250 mm long rebar with a \varnothing of 10 mm was used as anode. However, only the central 50 mm was exposed to the concrete to act as anodic area. Therefore, the sides were protected by coating both ends with two layers of cement paste ($W/C = 0.4$) and two layers of epoxy resin. For both the anode and the cathode, an electrical connection to the exterior was provided by insulated copper wires. Therefore, a copper screw was welded onto the reinforcement and a ring shaped cable shoe was placed on the copper wire. Two brass nuts were used to fasten the cable shoe to the screw. Afterwards, these electrical connections were coated with epoxy resin to avoid galvanic corrosion. As structural reinforcement inert, non-corrosive and non-conductive glass fiber reinforcement bars with a \varnothing of 6 mm were used which continued along the entire length of the beams. These glass fiber bars (Aslan 100 GFRP) contained glass fiber type E impregnated with vinyl ester resin.

The WRA and/or CI were provided inside the beams by adding two layers of capsules, one above and one underneath the anodic steel bar with six capsules in each layer (Figure 1). The capsules were fixed with glue on plastic wires which were attached to the walls of the mould. Also triangular notches with a height of 4 mm were provided inside the moulds to make sure that the crack originated in the center of the prism. The beams were cast with the concrete mixtures described in Table 2 in three consecutive layers with 30 seconds compaction on the vibration table intermediately. After casting the beams, they were stored in an air-conditioned room with a temperature of 20°C and a relative humidity of at least 95%. After 24 hours, the beams were demoulded and stored in the aforementioned room until the age of 28 days. For each series (Table 3) three beams were prepared.

Table 2. Mix composition of the concrete mixtures.

Constituent	Composition [kg/m ³]	
	Batch 1	Batch 2
Sand 0/4	696	696
Gravel 2/8	502	502
Gravel 8/16	654	654
Cement CEM I 52.5 N	318	318
Fly ash	56	56
Water	153	142
Ferrogard 901 S	-	12

Table 3. Test series used for the corrosion measurements.

Code	(Un)cracked	Encapsulated products	Admixed products
UN	Uncracked	-	-
CR	Cracked	-	-
B	Cracked	MasterProtect 8000 CI	-
S	Cracked	Ferrogard 903 Plus	-
SF	Cracked	Sikagard 705 L	Ferrogard 901 S
N	Cracked	Sodium nitrite	-

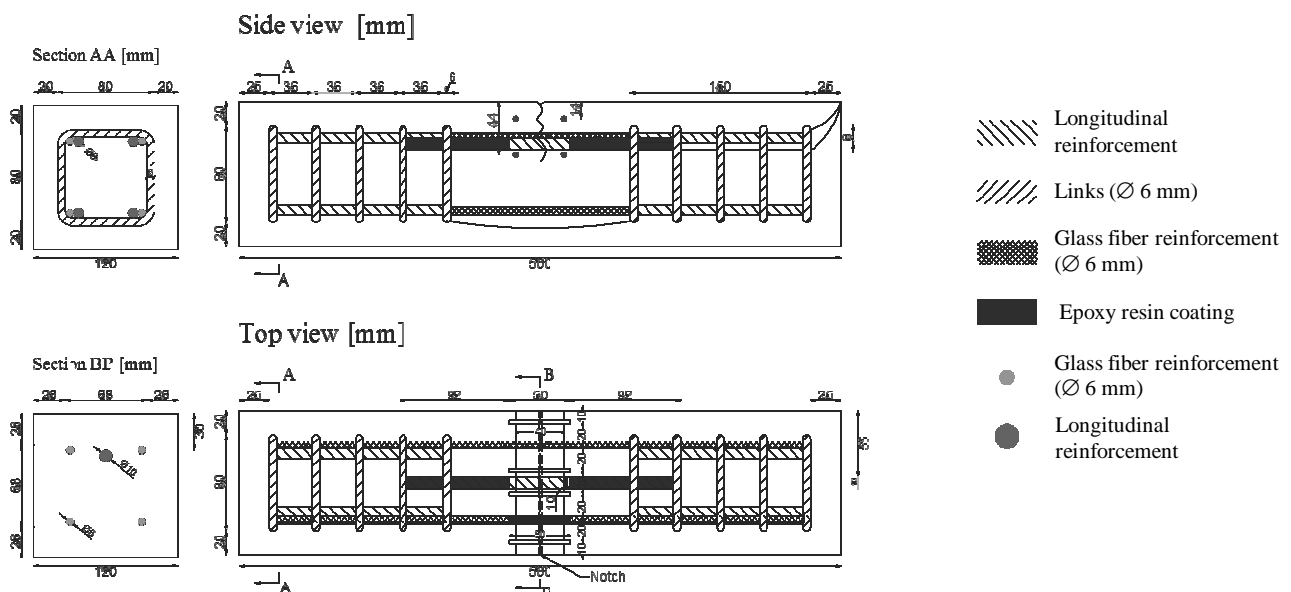


Figure 1. Preparation of the concrete beams (with embedded capsules) used for the corrosion measurements [22, 23].

Methods

Crack formation. It was aimed to create cracks with a width of 300 μm . This was done by means of a three-point bending test at the age of 28 days. Therefore, the concrete beams were placed with their notch at the top onto a central cylindrical steel bar with a diameter of 40 mm which was placed onto an I-shaped profile and stabilized by two hollow square steel profiles at each side of the beam with a width of 30 mm and a thickness of 3 mm. These hollow profiles were connected with screw thread so manual tightening of the screws induced three-point bending of the beams. During tightening of the screws and thus cracking of the beams, attention was paid to hear the capsules break. Once the desired crack width was obtained, stainless steel wires with a diameter of 450 μm were positioned inside the crack before unloading of the beams to maintain the crack width after

unloading. During the three-point bending test, some additional cracks were noticed, which could not be avoided in order to achieve a sufficient width of the central crack. These unwanted cracks were later filled with a cement slurry of 100 g/l through injection with a syringe. The cracks positioned in the zone with NaCl solution (see later) were also covered with aluminum butyl tape of 5 mm width to have no direct ingress of chlorides from the surface into these cracks. After the bending test, the beams were positioned with the cracked face facing downwards, giving the WRA and/or the CI the opportunity to flow into the crack. After 24 hours, the crack width of the realistic cracks was measured with a stereomicroscope.

Crack repair. Crack healing was obtained in an autonomous way. At the moment the beams were bent to create the cracks, the glass capsules were broken. Due to breakage of the glass capsules the WRA and/or CI were released inside the crack.

Corrosion measurements. As only the top (cracked) and the bottom surface of the beams would be exposed to the environment, the other faces were covered with aluminum butyl tape. On the cracked surface, three basins were installed with a sodium chloride solution (33 g/l NaCl, 1.5 m% NaCl) in the middle compartment (length 100 mm) and a calcium hydroxide solution (1.15 g/l CaOH₂) in the outer compartments. The edges of the basins were made with aluminum butyl tape and the subdivisions with PVC plates. Silicon resin was used to ensure the liquid tightness at the edges of the basins. The specimens were subjected to wet/dry cycles of 3.5/3.5 days. At the end of each wetting period, the open circuit potential (OCP) of the anode (E_A) and the cathode (E_C) was measured. Therefore, a saturated calomel reference electrode was used and placed in the central reservoir in the middle of the transverse notch. From these measurements the driving potential was derived as the difference of E_A and E_C . In addition, the corrosion potential was measured, together with the linear polarization resistance of the anode and the cathode. Also IR drop measurements and electrochemical impedance spectroscopy measurements were performed at regular intervals, however these results are not reported in this publication. After the measurements, the sodium chloride and the calcium hydroxide solutions were removed from the basins. Solutions were refreshed every time the basins were filled again. The experiment started right before the first wetting cycle, when the wire of the anodic and cathodic reinforcement were connected, and lasted for 12 weeks. The anode and cathode remained continuously clamped together outside the beam and the corrosion current was measured on a daily basis by connecting the anodic and cathodic external connection wire to a multimeter (ISO-Tech IDM 71) with a resolution of 0.1 μ A.

Results

Corrosion measurements. Before and during the corrosion process, different measurements were performed, as presented in the following sections.

Crack widths. The crack width for every beam was measured and the general average crack width amounted to 275 μ m with the minimum and maximum crack width being equal to 204 and 370 μ m, respectively. The obtained widths of the realistic cracks approached well the aimed value of 300 μ m.

Current monitoring. Current monitoring provides an immediate indication of the macro-cell corrosion condition of the beams. However, micro-cell corrosion will also occur which is not measured in this way. The only way to assess micro-cell corrosion is by demolishing the concrete beams and investigating the state of the reinforcement which is only foreseen in a later stage of this study. Therefore, all further conclusions are based on the measured part of the macro-cell corrosion. During the wet cycles (Figure 2), increases in current are noticed after which a decrease is noticed when the dry cycle starts. This was most pronounced for test series where high currents developed. For beams with lower current values measured, an almost steady invariant behavior was found.

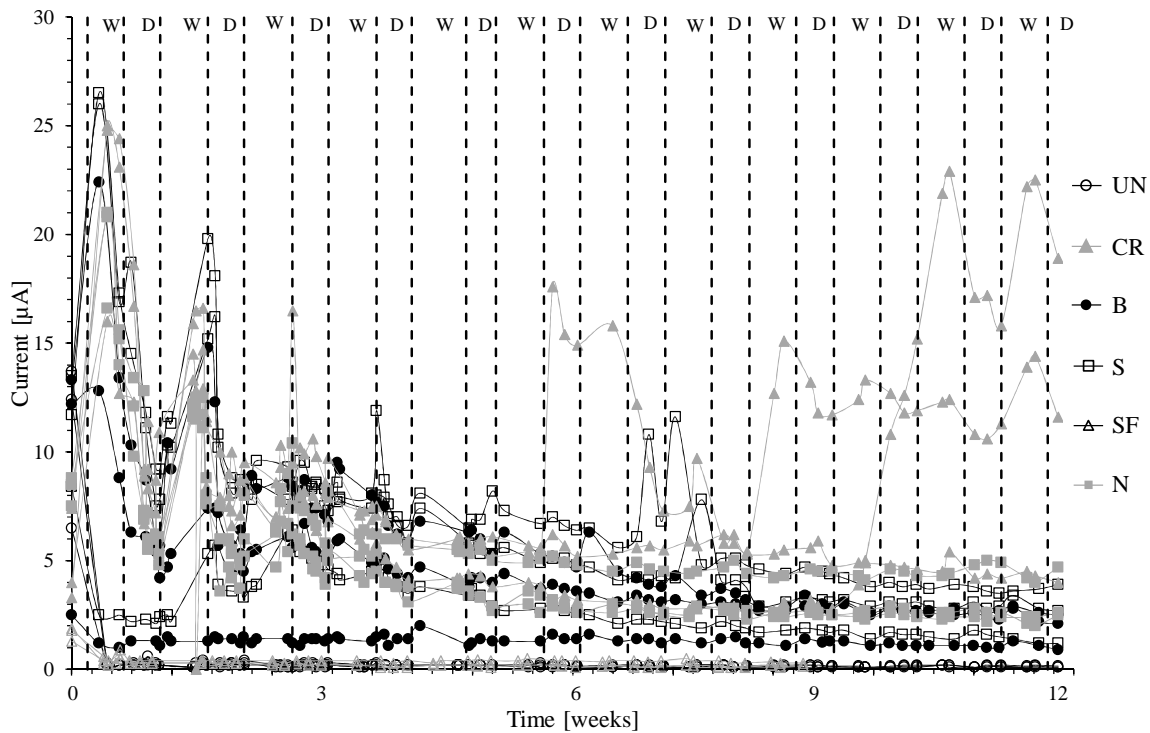


Figure 2. Evolution of the corrosion current over time.

First of all, the difference in behavior between cracked (CR) and uncracked, untreated (UN) concrete was clearly visible. Almost zero current measurements were obtained for the uncracked specimens, ranging between 0.1 and 0.6 μA . For the cracked beams, much higher currents were measured. One beam of the CR series showed a peak of 18 μA after 6 weeks of exposure and together with another beam of that series high current values (15 and 23 μA) were obtained near the end. While the series where the rebar was protected through release of embedded WRA and/or CI did not show these very sharp increases in current, compared to the UN series higher values for the current were measured, except for the SF series. Although the authors are aware of the fact that sound conclusions can only be drawn when comparing the current density, as the experiments are still going on, conclusions were drawn based on the measured currents. As soon as a certain current / current density is measured this indicates that corrosion is going on so it can be concluded that for none of the aforementioned samples corrosion was completely omitted. Only for the series SF where the WRA Ferrogard 901 S was admixed to the matrix and the CI Sikagard 705 L was embedded inside capsules, the corrosion current was negligible.

Driving potential. The open circuit potential (OCP) of the anode and the cathode were measured on a weekly basis. The difference between the OCP of anode and cathode results in the driving voltage of the corrosion process, which is a basic parameter to assess the reinforcements' corrosion state [23]. Consequently, larger values are an indication of a more active corrosion cell. In Figure 3 the obtained driving voltages at week 9 are shown together with the measured currents at that time. The lowest average driving voltage was noticed for the test series with encapsulated WRA in combination with mixed in CI (SF), being equal to 130 mV. A slightly higher mean driving voltage was noticed for the uncracked series (155 mV). It can thus be concluded that the series SF performed well, since a similar performance as for the uncracked beams was noticed. This is also confirmed when looking at the graph showing the measured currents at week 9. Also the series B resulted in average driving voltages which did not differ significantly from the values obtained for the uncracked series. The series which did only contain encapsulated WRA (without mixed in CI), series S, and the series with encapsulated sodium nitrite (N) resulted in driving voltages which were significantly higher compared to the values obtained for the uncracked series. For the series N, there

was no significant improvement in the obtained average driving voltage of 290 mV compared to the mean driving voltage obtained for the series with untreated cracks (CR) being 370 mV.

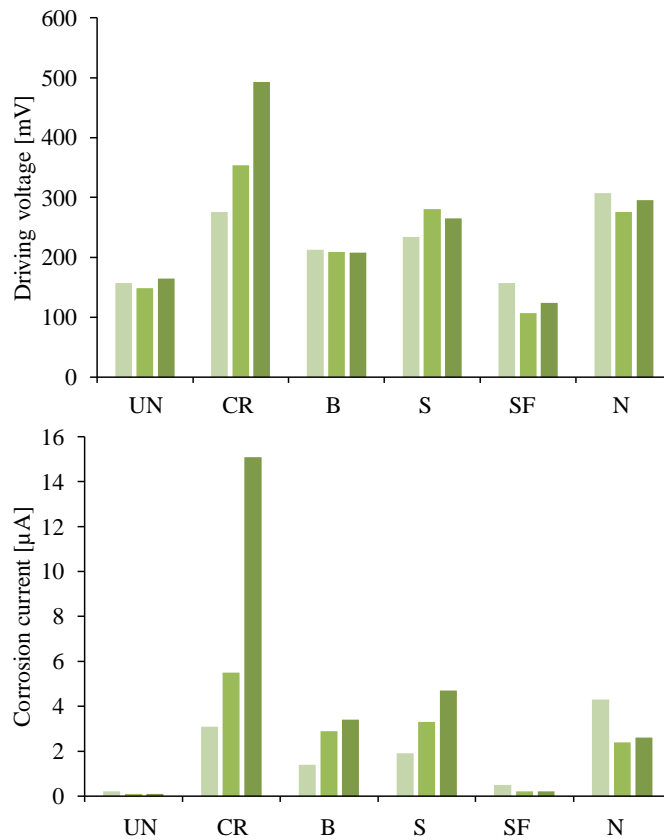


Figure 3. Driving voltage and corrosion current at week 9 of the corrosion measurements.

Conclusions

It can be concluded that the local release of WRA and/or CI may reduce the corrosion current. Best results were obtained when the combination of a product with water repellent properties and corrosion inhibiting properties was provided. This was the case for the series B, where the product MasterProtect 8000 CI was released from the embedded capsules, as this product has both water repellent and corrosion inhibiting properties. In addition, for series SF, where the WRA Sikagard 705 L was encapsulated and the CI Ferrogard 901 S was mixed in, promising results were obtained. Series B performed somewhat worse with regard to the current measurements but the obtained mean driving voltage did not differ significantly from the uncracked series. For the series SF both, the current measurements and the driving voltages were comparable to those obtained for uncracked samples.

The other test series under investigation, with encapsulation of the CI Ferrogard 903 Plus (S) or encapsulation of sodium nitrite (N), only showed a slight improvement in the protection of the reinforcement steel. The current measurements during the corrosion experiment differed from zero and the driving potential measured after 9 weeks testing was significantly different from the one obtained for uncracked samples.

The results of this experimental study indicate that providing WRA and/or CI via embedded capsules is a promising technique to overcome current problems related to the specific application techniques of these products. However, in order to efficiently reduce the risk for corrosion a combination of both a WRA and a CI needs to be provided.

While it is the aim to continue the electrochemical measurements on the concrete beams for a longer period in time, finally we will break open the concrete beams to perform a microscopic analysis of the status of the rebars.

Acknowledgements

Financial support from the Research Foundation Flanders (FWO-Vlaanderen) for this study (project number 12A3314N) is gratefully acknowledged.

References

- [1] R. Javaherdashti, *Microbiologically influenced corrosion: an engineering insight*. Springer Science & Business Media, 2008.
- [2] K. Van Tittelboom, N. De Belie, D. Van Loo, P. Jacobs, Self-healing efficiency of cementitious materials containing tubular capsules filled with healing agent. *Cement and concrete composites*, 33(4), 497-505, 2011.
- [3] K. Van Tittelboom, D. Snoeck, P. Vontobel, F.H.. Wittmann, N. De Belie, Use of neutron radiography and tomography to visualize the autonomous crack sealing efficiency in cementitious materials. *Materials and Structures*, 46(1-2), 105-121, 2013.
- [4] J. Pacheco, *Corrosion of steel in cracked concrete*, PhD dissertation, TUDelft, 2015.
- [5] P.P. Win, M. Watanabe, A. Machida, Penetration profile of chloride ion in cracked reinforced concrete. *Cement and Concrete Research*, 34 (7), 1073-1079, 2004.
- [6] S. Jacobsen, J. Marchand, L. Boisvert, Effect of cracking and healing on chloride transport in OPC concrete. *Cement and Concrete Research*, 26 (6), 869-881, 1996.
- [7] N. Gowripalan, V. Sirivivatnanon, C.C. Lim, Chloride diffusivity of concrete cracked in flexure, *Cement and Concrete Research*, 30 (5), 725-730, 2000.
- [8] M. Ismail, A. Toumi, R. François, Effect of crack opening on the local diffusion of chloride in cracked mortar samples. *Cement and Concrete Research*, 38 (8-9), 1106-1111, 2008.
- [9] A.M. Vaysburd, P.H. Emmons, Corrosion inhibitors and other protective systems in concrete repair: concepts or misconcepts. *Cement and Concrete Composites*, 26 (3):255-263, 2004.
- [10] R. Cagné, R. François, P. Masse, Chloride penetration testing of cracked mortar samples, *Proc. Of 3rd International Conference of Concrete under Severe Conditions*, University of British Columbia, Vancouver, Canada, 198-205, 2001.
- [11] E. Schlangen, I.S. Yoon, M.R. De Rooij, Measurement of chloride ingress in cracked concrete, *Proc. Of International RILEM Workshop on Transport Mechanisms in Cracked Concrete*, Ghent, 2007.
- [12] K. Audenaert, G. De Schutter, L. Marsavina, The influence of cracks on chloride penetration in concrete structures – Part I: Experimental evaluation, *Transport Mechanisms in Cracked Concrete*. Eds. K. Audenaert, L. Marsavina, G. De Schutter, 13-18, 2007.
- [13] L. Marsavina, K. Audenaert, G. De Schutter, N. Faur, N.D. Marsavina, Experimental and numerical determination of the chloride penetration in cracked concrete, *Construction and Building Materials*, 23, 264-274, 2008.
- [14] P. Montes, T.W. Bremmer, D.H. Lister, Influence of calcium nitrite inhibitor and crack width on corrosion of steel in high performance concrete subjected to a simulated marine environment, *Cement and Concrete Composites*, 26: 243-253, 2004.

- [15] A. Scott, M.G. Alexander, The influence of binder, cracking and cover on corrosion rates of steel in chloride-contaminated concrete, *Magazine of Concrete Research*, 59 (7), 495-505, 2007.
- [16] M.B. Otieno, H.D. Beushausen, M.G. Alexander, Modelling corrosion propagation in reinforced concrete structures – A critical review. *Cement & Concrete Composites*, 33, 240-245, 2011.
- [17] C. Andrade C, C. Alonso, Corrosion rate monitoring in the laboratory and on site, *Construction and Building materials*, 10(5), 315-328, 1996.
- [18] A. Beeby, Cracking, cover and corrosion of reinforcement. *Concrete International*, 5 (2), 35-40, 1983.
- [19] EN 1504-9, Products and systems for the protection and repair of concrete structures - Definitions, requirements, quality control and evaluation of conformity - Part 9: General principles for the use of products and systems.
- [20] L. Bertolini, B. Elsener, P. Pedferri, E. Redaelli, R. Polder, *Corrosion of steel in concrete: Prevention, diagnosis, repair*, wiley-VCH Verlag GmbH & Co. KGaA, 2013.
- [21] Y.G. Zhu, S.C. Kou, C.S. Poon, J.G. Dai, Q.Y. Li, Influence of silane-based water repellent on the durability properties of recycled aggregate concrete, *Cement and Concrete Composites*, 35 (1), 32-38, 2013.
- [22] F. Hiemer, S. Keßler, C. Gehlen, Reinforcement corrosion behavior in bending cracks after short-time chloride exposure. In *Proceedings Concrete Repair, Rehabilitation and Retrofitting IV – Dehn et al. (Eds) © 2016 Taylor & Francis Group, London, ISBN 978-1-138-02843-2, Leipzig, 2015.*
- [23] F. Hiemer, S. Keßler, C. Gehlen, Development of chloride induced reinforcement corrosion in cracked concrete after application of a surface protection system, In *Proceeding Concrete Solutions 6th International Conference on Concrete Repair, Thessaloniki, 20-22 June 2016.*